Water Research 302 (2026) 126057

Contents lists available at ScienceDirect

Water Research

journal homepage: www.elsevier.com/locate/watres

Glycine-mediated microbial interactions in biological phosphorus removal systems

Agustina Ziliani [a,b,*], Patricia Bovio-Winkler [c], Martin Pabst [d], Angela Cabezas [e], Claudia Etchebehere [c], Hector A. Garcia [b], Carlos M. López-Vázquez [b], Damir Brdjanovic [b], Mark C.M. van Loosdrecht [d], Francisco J. Rubio-Rincón [b]

[a] Department of Environmental Microbiology, Swiss Federal Institute of Aquatic Science and Technology (Eawag), 8600, Dübendorf, Switzerland
[b] Department of Water Supply, Sanitation, and Environmental Engineering, IHE Institute for Water Education, Delft, The Netherlands
[c] Laboratorio de Ecología Microbiana, Instituto de Investigaciones Biológicas Clemente Estable, Montevideo, Uruguay
[d] Department of Biotechnology, Delft University of Technology, Delft, The Netherlands
[e] Instituto Tecnológico Regional Centro Sur, Universidad Tecnológica, Durazno, Uruguay

HIGHLIGHTS

- Glycine supported EBPR in a sequencing batch reactor.
- Phosphorus removal (20 mg PO_4-P L^{-1}) and DOC:P ratio (100:9.9) were achieved.
- Saccharimonadales were strongly enriched under glycine feeding.
- Glycine metabolism potential was shared between fermentative and PAO-like taxa.

GRAPHICAL ABSTRACT

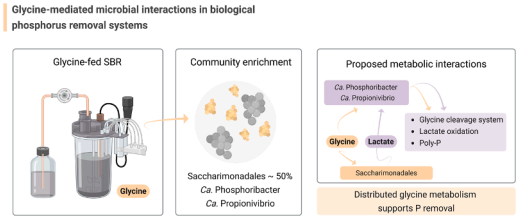

ARTICLE INFO

Keywords:
Enhanced biological phosphorus removal
Glycine metabolism
Saccharimonadales
Ca. Phosphoribacter
Metagenomics

ABSTRACT

Amino acids are less studied substrates in enhanced biological phosphorus removal (EBPR) systems. Glycine, a prevalent amino acid in wastewater, was used in this study to evaluate its role in EBPR processes. We operated a sequencing batch reactor (SBR) for over three months with glycine as the sole carbon source to investigate phosphorus removal performance and microbial dynamics using chemical and molecular analyses. The reactor supported EBPR activity, with glycine enabling anaerobic phosphorus release followed by aerobic uptake. The dissolved organic carbon to phosphorus (DOC:P) removal ratio of 100:9.9 closely matched values reported for systems dominated by polyphosphate-accumulating organisms (PAOs), and net phosphorus removal (20 mg PO_4-P L^{-1}) fell within the range reported for laboratory-scale EBPR systems fed with mixed carbon sources. Community analyses showed enrichment of Saccharimonadales alongside putative PAOs, including *Ca.* Phosphoribacter and *Ca.* Propionivibrio. Genome-resolved analyses indicate distinct but complementary metabolic potentials, including glycine transformation and lactate-related pathways, suggesting distributed carbon processing within the community. Together, these findings expand the understanding of amino acid utilization in EBPR systems and identify potential metabolic linkages that influence phosphorus removal under glycine-fed conditions.

* Corresponding author.
E-mail address: agustina.ziliani@eawag.ch (A. Ziliani).

https://doi.org/10.1016/j.watres.2026.126057
Received 28 December 2025; Received in revised form 24 April 2026; Accepted 1 May 2026
Available online 4 May 2026

1. Introduction

Effective phosphorus removal in wastewater treatment is essential to prevent eutrophication and associated adverse ecological impacts in receiving waterbodies (Bunce et al., 2018). Enhanced Biological Phosphorus Removal (EBPR) is widely applied for this purpose (Barnard et al., 2017). However, wastewater influents contain a complex mixture of organic matter, including proteins and their degradation products, which can influence EBPR performance. As proteins are hydrolyzed, amino acids are released and become available to the microbial community, potentially affecting metabolic pathways involved in phosphorus removal (Nielsen et al., 2012; Thomson et al., 2025).

Polyphosphate-accumulating organisms (PAOs) are the key drivers of phosphorus removal and comprise a phylogenetically diverse group of microorganisms with different metabolic strategies (Ruiz-Haddad et al., 2024). Conventional PAOs, such as *Candidatus* Accumulibacter and members of the genus *Dechloromonas*, accumulate polyhydroxyalkanoates (PHA) from available carbon sources, such as volatile fatty acids (VFAs) and glucose, coupling polyphosphate hydrolysis to carbon uptake (Oyserman et al., 2016; Ziliani et al., 2023). In contrast, fermentative PAOs, including *Candidatus* Phosphoribacter (formerly *Tetrasphaera*), can utilize amino acids and sugars and may rely on fermentative pathways to support polyphosphate cycling (Ruiz-Haddad et al., 2024; Singleton et al., 2022). The genus *Ca.* Phosphoribacter was recently reclassified based on genome-resolved phylogeny (Singleton et al., 2022). Throughout this manuscript, we use the updated designation *Ca.* Phosphoribacter, while retaining the original genus name when referring to studies published before this reclassification. Additional PAO-related taxa display metabolic flexibility, enabling storage of diverse intracellular compounds (Kawakoshi et al., 2012; Rubio-Rincón et al., 2017). This metabolic heterogeneity among PAOs contributes to their resilience in fluctuating wastewater environments and suggests that amino acid-rich conditions may alter PAO community structure and influence phosphorus removal dynamics (Confer et al., 1995).

Among amino acids, glycine has been reported to influence EBPR performance (Marques et al., 2017; Nguyen et al., 2015; Oyserman et al., 2016; Tian et al., 2022). Nguyen et al. (2015) reported that glycine could trigger phosphorus release and uptake in *Tetrasphaera*-enriched systems. However, other studies reported lower phosphorus release rates and atypical kinetics when glycine was supplied relative to other amino acids or classical VFA substrates such as acetate and propionate (Qiu et al., 2020; Tian et al., 2022). These contrasting results indicate that the role of glycine in EBPR systems remains unresolved and may depend on microbial composition and metabolic interactions rather than substrate chemistry alone.

Microbial cross-feeding is a determinant of EBPR stability and performance. Fermentative microorganisms can convert substrates into low-molecular-weight intermediates that are subsequently used by PAOs, creating metabolically coupled communities (Elahinik et al., 2023, 2022; Marques et al., 2017). Members of the order Saccharimonadales (formerly TM7) are obligate fermenters frequently detected in wastewater treatment plants (Albertsen et al., 2013). Although typically present at low abundance, their fermentative metabolism suggests a potential role in carbon redistribution under amino acid-rich conditions. However, their interactions with PAOs during glycine-driven EBPR have not been investigated, and the extent to which they contribute to substrate transformation and phosphorus removal remains unclear.

In this study, we operated a sequencing batch reactor (SBR) for over three months using glycine as the sole carbon source to evaluate EBPR performance and the enriched microbial community. Using chemical analyses, metagenomics, metaproteomics, and fluorescence *in situ* hybridization (FISH), we examined phosphorus removal efficiency and community composition, with particular attention to the enrichment of Saccharimonadales and their potential metabolic interaction with PAOs under sustained glycine-fed conditions.

2. Materials and methods

2.1. Sequencing batch reactor (SBR) operation overview

We utilized an Applikon double-jacketed SBR with a 2.5 L working capacity, controlled by BioXpert software and an Applikon ADI 1030 bio-controller. The inoculum consisted of a 1:1 (v/v) mixture of activated sludge from the Harnaschpolder biological nutrient removal plant (Delft, The Netherlands) and sludge from the Center for Microbial Communities at Aalborg University (Department of Chemistry and Bioscience, Aalborg, Denmark). The SBR operated in 8-h cycles, comprising 3.5 h of anaerobic, 3 h of aerobic, and 1.5 h of settling and effluent withdrawal phases. Each cycle began with the addition of 1.25 L of synthetic medium. Each liter of medium contained 400 mg C (as glycine), 50 mg PO_4^{3-} − P, 28 mg NH_4^+-N, 50 mg SO_4^{2-}, 19 mg K^+, 15 mg Mg^{2+}, 4 mg Ca^{2+}, 1 mg yeast extract, 20 mg N-allylthiourea (ATU), and 300 μL of trace elements solution (Smolders et al., 1994), as previously reported by Rubio-Rincón et al. (2019).

At the end of the aerobic phase, approximately 55 mL of well-mixed liquor was withdrawn for sludge wasting (WAS) before settling. These operational settings resulted in hydraulic retention times (HRT) and sludge retention times (SRT) of 16 h and 15 d, respectively, with an aerobic SRT of 5.6 d, following the approach of Rubio-Rincón et al. (2019).

We maintained the pH at 7.0 ± 0.1 using 0.4 M HCl or 0.4 M NaOH as needed. Temperature control was achieved at 20 ± 1 °C using a Lauda-Brinkmann RE106 water bath chiller (Delran) with water recirculation through the reactor's double jacket. Anaerobic conditions were induced by bubbling dinitrogen gas for the first 25 min of each cycle. We set the overhead mixer to 300 rpm throughout both the anaerobic and aerobic phases while maintaining dissolved oxygen (DO) at 20% by adding compressed air. The reactor was operated for approximately 100 d.

2.2. Evaluating reactor performance

For routine chemical monitoring, we collected samples twice per week at three defined timepoints within a single cycle: (i) at the beginning of the anaerobic phase, immediately after influent feeding (5 min), (ii) at the beginning of the aerobic phase, and (iii) at the beginning of the settling phase while stirring was still active. At each timepoint, 5 mL of mixed liquor was withdrawn, resulting in 15 mL per monitoring day. We used these samples for analyses of ammonia, orthophosphate, dissolved organic carbon (DOC), and acetate. We conducted measurements on the same day using standard methods (APHA et al., 2005). We quantified volatile fatty acids (VFAs) using a Varian 460 gas chromatograph (Nieuwegein), with propionic acid as the internal standard. Once per week, we stored 1.5 mL of the sample taken at the end of the anaerobic phase at - 20 °C for subsequent FISH and genomic DNA extraction. We did not perform separate sampling events for molecular analyses, instead using aliquots from the routine monitoring.

We measured the weekly concentration of mixed liquor suspended solids (MLSS) and mixed liquor volatile suspended solids (MLVSS) using three independent 10 mL samples. When no significant changes in these parameters (greater than 1%) were observed over at least three SRTs, we considered the reactor to be in pseudo steady-state. At that point, we conducted cycle studies to further evaluate carbon utilization. We determined the sampling schedule based on pH and DO trends in the software cycle results. Sampling consisted of one sample every 5 min for the first hour of both anaerobic and aerobic phases, followed by one sample every 20 min thereafter. In total, we collected 38 samples per cycle study for chemical analyses, in addition to samples for MLVSS/MLSS analysis at the start and end of each operating phase. We did not withdraw mixed liquor during the following five cycles to compensate for sludge loss.

2.3. Parameter estimation: stoichiometry and kinetics

We calculated the kinetic parameters using the linear regression method defined by Smolders et al. (1995), which requires at least five experimental points. The estimated parameters included the maximum specific anaerobic phosphate release rate, maximum specific aerobic phosphate uptake rate, and maximum specific anaerobic DOC consumption rate. We further derived stoichiometric parameters for net phosphate release and the phosphate released per carbon consumed ratio (P/C). We accounted for phosphate release attributed to maintenance factors by subtracting it from the total observed phosphate release. These calculations factored in concentration values once the carbon source was depleted.

2.4. Amplicon sequencing

We extracted genomic DNA (gDNA) using the QIAamp® PowerFecal® DNA kit (QIAGEN) from the weekly monitoring samples and quantified it using the Qubit™ 3.0 Fluorometer. Amplicon sequencing was conducted by Macrogen Inc. (Seoul, Korea) on an Illumina MiSeq platform, using the Illumina Reagent Kit v2 and primers 341F (5′-CCTACGGGNGGCWGCAG-3′) and 805R (5′-GACTACHVGGGTATCTAATCC-3′) designed specifically for the V3-V4 regions of bacteria (Herlemann et al., 2011). We sequenced the inoculum sample and a representative reactor sample collected at pseudo steady-state (operation day 75).

We processed sequencing data using QIIME2 and DADA2 to generate amplicon sequence variants (ASVs), and we assigned taxonomy using the MiDAS 4.8.1 database (Callahan et al., 2016; Dueholm et al., 2022). Detailed bioinformatic parameters are described in Text S1.

2.5. Fluorescence in situ hybridization (FISH) analysis

We performed weekly FISH analyses to monitor the presence and relative abundance of key microbial groups during reactor operation. We analyzed the samples from pseudo steady-state onwards (approximately day 50). We fixed samples following established protocols for Gram-negative and Gram-positive bacteria (see Text S2 for detailed procedures).

We targeted PAOs with probes PAO 462, PAO 651, and PAO 846, which together cover approximately 89% of *Ca.* Accumulibacter-related bacteria (Crocetti et al., 2000). Because *Ca*. Propionivibrio was identified as abundant in the reactor community based on 16S rRNA gene sequencing and metaproteomic analysis, we additionally evaluated samples using PAO 651 independently to reduce potential overestimation due to cross-hybridization (Albertsen et al., 2016). The PAO 651 probe provides approximately 71% coverage of *Ca.* Accumulibacter and yields a more conservative estimate of its abundance. We targeted members of the genus *Tetrasphaera* using the Tet2-842 probe and glycogen-accumulating organisms (GAO) with probes GAOQ 431 and GAOQ 989 (Crocetti et al., 2002; Nguyen et al., 2011) (Table S1).

We performed observations with an Olympus BX51 microscope and quantified abundances based on 20 randomly selected fields of view.

2.6. Metaproteome analysis

We performed the metaproteomic analysis as previously described (Kleikamp et al., 2023). We used biomass samples collected after the reactor reached pseudo steady-state. We extracted proteins, digested them with trypsin (Promega), and analyzed peptides using one-dimensional shotgun proteomics on an EASY nano-LC 1200 system coupled to a QE Plus Orbitrap mass spectrometer (Thermo Fisher Scientific).

We searched mass spectra against a protein database constructed from open reading frames (ORFs) predicted from the metagenomic assemblies generated from the same reactor biomass samples analyzed in this study. We processed raw data using PEAKS StudioX (Bioinformatics Solutions Inc.) and assigned functional annotations using KEGG orthologies via BlastKOALA (Kanehisa et al., 2016; Kanehisa and Goto, 2000). Detailed extraction procedures, database construction, and data-processing parameters are provided (Text S3). We deposited the mass spectrometry proteomics data to the ProteomeXchange Consortium via the PRIDE partner repository with the dataset identifier PXD077488.

2.7. Metagenomic analysis

We performed shotgun metagenomic sequencing on the Illumina NovaSeq 6000 platform (2 × 150 bp) by Novogene Corporation Inc. (Sacramento, CA). We extracted DNA from triplicate biomass samples collected during pseudo steady-state operation (after operational day 50) and pooled them before sequencing.

We quality-filtered raw reads and assembled contigs. We generated metagenome-assembled genomes (MAGs) through binning and refinement, and assessed their completeness and contamination. We assigned taxonomy with GTDB-Tk v1.7.0 and the Genome Taxonomy Database (GTDB) r214 (Chaumeil et al., 2020; Parks et al., 2020, 2015). Finally, we reconstructed metabolic pathways using KEGG orthologies (Kanehisa and Goto, 2000). We quantified gene-level abundance by mapping quality-filtered reads to the reconstructed MAGs and calculating reads per kilobase per million mapped reads (RPKM) for KEGG-annotated genes to normalize gene length and sequencing depth. The detailed bioinformatic workflow is described in the Supplementary material (Text S4). Raw amplicon and metagenomic sequences are available under NCBI BioProject PRJNA809015.

3. Results

3.1. Reactor operation and EBPR profile

We operated the SBR continuously for over 90 d, reaching a pseudo steady-state around day 50, corresponding to 3.3 solid retention times (SRTs). The MLVSS/MLSS ratio fluctuated between 0.82 and 0.98 (Fig. S1). Process monitoring confirmed stable operational conditions throughout the experimental period. The pH was tightly controlled between 6.88 and 7.16 (7.02 ± 0.08), and temperature remained stable at 20.6 ± 0.2 °C. During anaerobic phases, oxidation-reduction potential (ORP) values decreased to approximately –93 mV, while during aeration, ORP increased to positive values up to 82 mV, confirming clear redox separation. Representative cycle profiles of pH, DO, and ORP during pseudo steady-state operation are shown in Fig. S2.

Routine monitoring across reactor operation showed sustained phosphorus transformation capacity over time (Fig. 1A). During pseudo steady-state operation, anaerobic phosphorus release ranged from 1 to 20 mg PO_4-P L^{-1}, while aerobic phosphorus uptake ranged from 1 to 23 mg PO_4-P L^{-1}, and net phosphorus removal varied from 0 to 20 mg PO_4-P L^{-1}. DOC measurements taken at phase transitions showed substantial depletion during the anaerobic phase under pseudo steady-state conditions (Fig. S3). The maximum C:P removal ratio reached 100:9.9 (mg C mg^{-1} PO_4-P), calculated using measured DOC values. The phosphate biomass fraction (f_P) was 0.26 mg P mg^{-1} VSS, and an overall growth yield of 0.26 g VSS g^{-1} COD was obtained, consistent with values typically reported for PAO cultures (Smolders et al., 1994).

Cycle studies provided additional insights into reactor performance over the anaerobic and aerobic phases of operation (Fig. 1B). During the anaerobic phase, the carbon consumption rate was 38 mg C g^{-1} VSS h^{-1}, correlating with an anaerobic phosphate release rate of 17 mg PO_4-P L^{-1} at 3.7 mg PO_4-P g^{-1} VSS h^{-1} (Table 1). The phosphate released per carbon consumed ratio was calculated as 0.09 (mg PO_4-P mg^{-1} C). A strong negative correlation was observed between phosphorus and DOC concentrations during this phase ($r = –0.971$, $p = 1.97 \times 10^{-9}$), indicating that as DOC decreased, phosphorus concentration increased. The

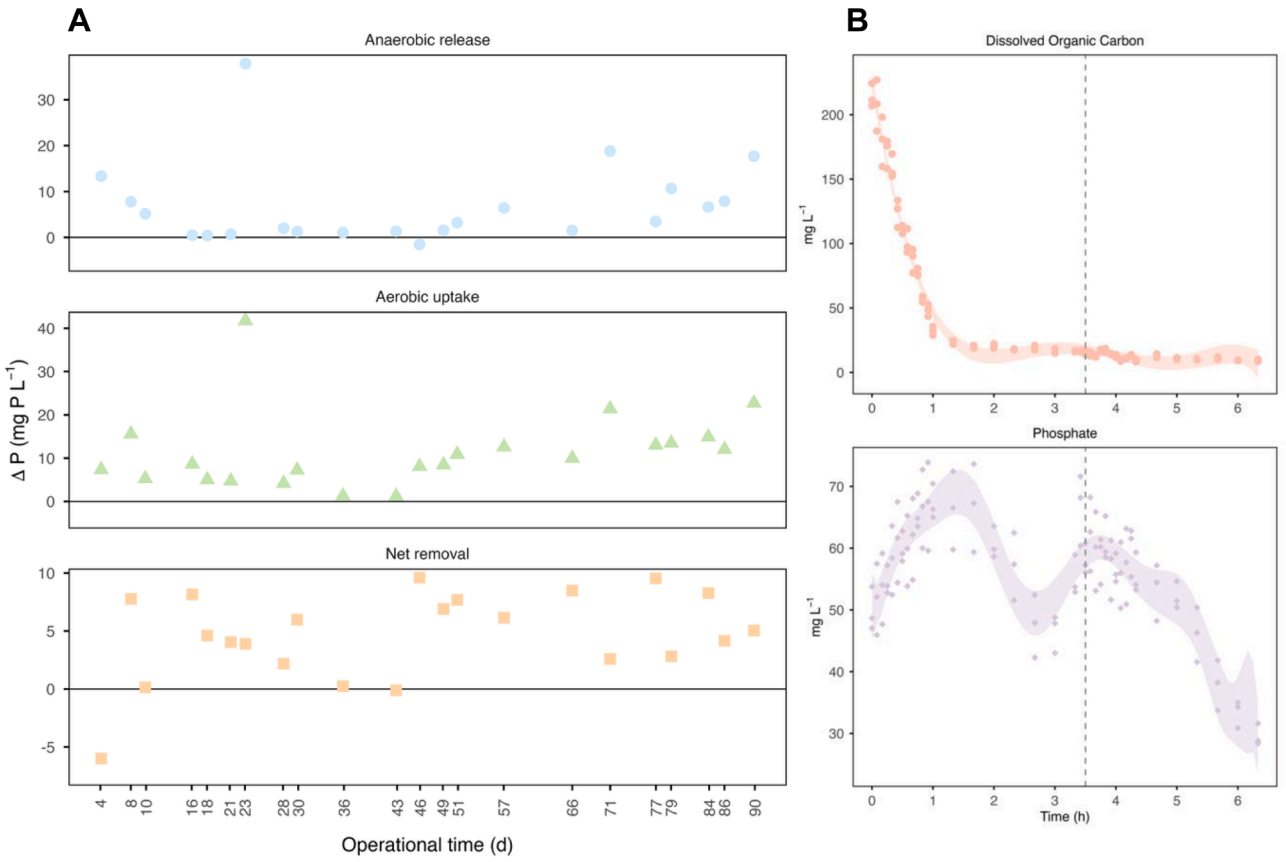

Fig. 1. A. Time-resolved phosphorus transformations during routine monitoring across reactor operation. Anaerobic phosphorus release was calculated as $\Delta P = P_{start\ aerobic} - P_{start\ anaerobic}$, aerobic uptake as $\Delta P = P_{start\ aerobic} - P_{end\ aerobic}$, and net phosphorus removal as $\Delta P = P_{start\ anaerobic} - P_{end\ aerobic}$. Positive values indicate phosphorus release, uptake, and net removal, respectively. B. Dissolved organic carbon (DOC) and phosphate concentration profiles during the cycle test performed under pseudo steady-state conditions. The dashed vertical line indicates the transition from anaerobic to aerobic phases. Shaded ribbons represent 95% confidence interval, and points represent triplicate measurements.

Table 1
Summary of stoichiometric and kinetic parameters for the cycle study. Values are reported as mean ± standard deviation (n = 3).

Anaerobic				Aerobic		Overall process		
net P release	max phosphate release rate	max DOC consumption rate	P/C ratio	net P uptake	max phosphate uptake rate	net P removal	growth yield	phosphate fraction (f_P)
mg L^{-1}	mg PO_4-P g^{-1} VSS h^{-1}	mg C g^{-1} VSS h^{-1}	mg P mg^{-1} C	mg L^{-1}	mg PO_4-P g^{-1} VSS h^{-1}	mg L^{-1}	g VSS g^{-1} COD	mg P mg^{-1} VSS
17.4 ± 4.5	3.7 ± 0.15	38.2 ± 2.6	0.096 ± 0.004	37.1 ± 1.6	3.4 ± 1.3	20.2 ± 1.3	0.26 ± 0.01	0.26 ± 0.04

correlation was calculated using the 15 data points before DOC reached its detection limit, beyond which the concentration remained stable. Then, in the aerobic phase, phosphorus uptake reached 37 mg PO_4-P L^{-1}, corresponding to a rate of 3.6 mg PO_4-P g^{-1} VSS h^{-1}. Overall, net phosphorus removal per cycle was 20 mg PO_4-P L^{-1}, accounting for 41% of the phosphorus initially fed (Table S2). Notably, the phosphorus profile differed from the sharp release-uptake pattern typically reported for acetate-fed EBPR systems. Maximum phosphate release occurred prior to complete anaerobic phase termination, likely reflecting rapid DOC depletion and distinct metabolic kinetics under glycine-fed conditions.

3.2. Microbial community characterization

We used 16S rRNA gene amplicon sequencing and fluorescence *in situ* hybridization (FISH) to characterize the composition and dynamics of microbial populations as the reactor transitioned from startup to pseudo steady-state conditions. Amplicon sequencing indicated an increase in the relative abundance of the Saccharimonadales order. Initially comprising 0.4% of the microbial community in the inoculum, these bacteria increased markedly, ultimately dominating the reactor's population at 52.1% (Fig. 2A). Bacteroidia, which includes the orders Chitinophagales and Bacteroidales, displayed nuanced changes. The former decreased from 10.6% in the inoculum to 6.1% in the reactor, while the latter increased from 2.5% to 8.1%. On the other hand, the Nitrospira class, known for its potential role in nitrogen cycling, decreased from 6.6% to absent in the reactor. Similar results were observed for the order Competibacterales, signaling shifts in functional microbial groups within the reactor.

Genus-level analysis provided a more detailed view of community shifts (Fig. 2B). In this regard, members of the order Saccharimonadales dominated the community, representing approximately 50.4% of the total relative abundance. Three distinct taxa affiliated with this order (*midas_f_728* and *midas_g_67*) were not detected in the inoculum but

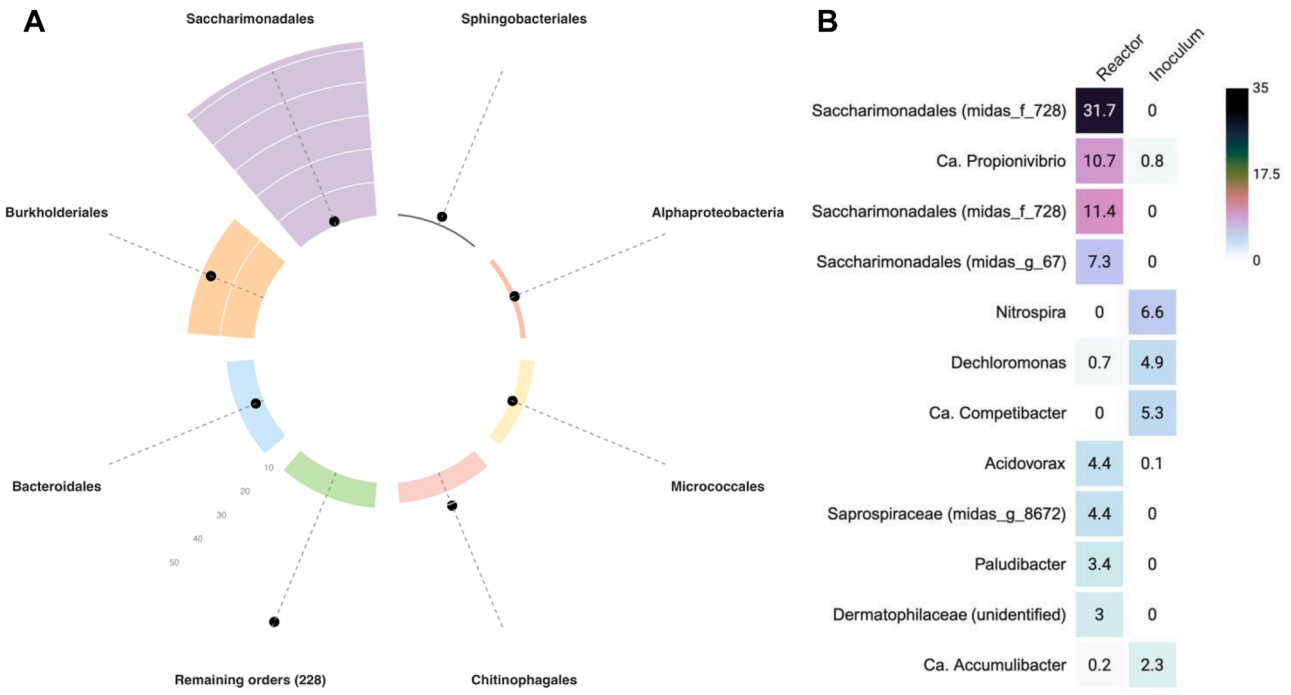

Fig. 2. A. Relative abundances of microbial orders in the reactor based on 16S rRNA gene amplicon sequencing data. Each bar represents a taxonomic order, with heights corresponding to their relative abundances in the community. Black data points indicate values from the inoculum. B. Heatmap of the most abundant bacterial taxa in the inoculum and reactor samples. Each row represents a taxon, with color intensity indicating relative abundance. When genus-level identification was not possible, the corresponding family (and order) names are shown.

became enriched during reactor operation. *Ca.* Propionivibrio also exhibited a notable increase, from 0.8% in the inoculum to 10.7% in the reactor. These results suggest that this genus may play an important role in reactor processes, possibly related to phosphorus removal or organic matter degradation. An unidentified genus of the family *Dermatophilaceae* (to which *Ca.* Phosphoribacter belongs) was also among the most abundant taxa detected by amplicon sequencing in the reactor. It should be noted that 16S rRNA gene amplicon sequencing does not reliably distinguish *Ca.* Phosphoribacter from closely related lineages within this family, as its recent delineation was based on genome-level phylogeny (Singleton et al., 2022). Finally, *Ca.* Accumulibacter, the most-studied organism in phosphorus removal systems, declined from 2.3 to 0.2%.

To complement these observations, we conducted FISH analyses targeting three main clusters: the PAO cluster (*Ca.* Accumulibacter), *Tetrasphaera*-related microorganisms, and the GAO cluster. Average values from weekly analyses during pseudo steady-state operation showed that the PAO cluster accounted for 22 ± 2% of the total community (Fig. S5 and Table S3). However, to address potential overestimation resulting from the prevalence of *Ca.* Propionivibrio, we also used the probe PAO651 independently (Albertsen et al., 2016). When using this probe alone, which targets 71% of the PAO cluster and reduces possible cross-hybridization with *Ca.* Propionivibrio, the relative abundance decreased to 4 ± 0.2%, which is closer to the low relative abundance of *Ca.* Accumulibacter observed in the 16S rRNA gene amplicon sequencing data (0.2%). These results indicate that the combined PAO probe set may have overestimated the abundance of *Ca.* Accumulibacter. *Tetrasphaera*-related organisms, which are also associated with phosphorus removal, accounted for 8 ± 0.5% of the community, underscoring their potential contribution to EBPR activity. The GAO cluster constituted 6 ± 0.4% of the microbial population.

We note that the amplicon-based community comparison between the inoculum and pseudo steady-state reactor was based on single samples from each condition. Although these samples provide a snapshot of community composition at key operational stages, they do not allow statistical assessment of variability. The observed enrichment trends should therefore be interpreted as indicative rather than definitive. Weekly FISH analyses during pseudo steady-state operation provided independent quantification of selected functional groups (*e.g.*, PAOs and GAOs), but did not allow temporal validation of all taxa identified by sequencing.

3.3. *Metagenomic profiling of the reactor's microbial community*

We also conducted a more in-depth analysis of the microbial population's functional potential using shotgun metagenomic sequencing. We pooled several samples of the reactor once it had reached pseudo steady-state conditions for this analysis.

We assembled and annotated a total of 91 metagenome-assembled genomes (MAGs) with varying levels of completeness. Among these, 32 MAGs exhibited a completeness level exceeding 80%, 14 surpassing the 95% completeness threshold (Tables S4 and S5). Of these 91 MAGs, we focused on the ones belonging to the most abundant members of the community, as seen with the 16S rRNA gene amplicon sequencing and FISH analyses, or those that contained specific genes of interest. We mainly explored the genetic components involved in glycine transformation, lactate-related metabolism, phosphorus accumulation, and the known pathways responsible for polyhydroxyalkanoate (PHA) and glycogen biosynthesis.

According to 16S rRNA gene profiles, Saccharimonadales dominated the reactor community (~ 50% relative abundance). Consistently, 8 MAGs affiliated with this order were recovered, four of which are high-quality drafts (> 97% completeness, < 5% contamination) (Bowers et al., 2017). These Saccharimonadales MAGs exhibited reduced genome sizes and low-GC content, characteristic of Patescibacteria. Across these MAGs, 83 KEGG modules were partially represented, although relatively few were complete. Core metabolic modules such as glycolysis, the ABC-2 type transport system, aminoacyl-tRNA biosynthesis, and the twin-arginine translocation (Tat) system were consistently detected.

Analysis of glycine metabolism revealed that canonical glycine cleavage system (GCS) genes (*gcvP, gcvT*, GCSH, and *lpd*) were not

detected in Saccharimonadales MAGs (Fig. 3). Enzymes associated with glycine to glyoxylate conversion and glycine transamination were also absent. However, glycine hydroxymethyl transferase (*glyA*), which converts glycine to serine, was present in most Saccharimonadales MAGs. Genes encoding serine deaminase (*ilvA*) and lactate dehydrogenase (LDH) were also detected, supporting potential conversion of serine to pyruvate and subsequently to lactate. Furthermore, the pathways leading to tryptophan biosynthesis and the conversion of pyruvate to acetyl-CoA were also identified.

The absence of a complete glycine cleavage system in Saccharimonadales MAGs raises uncertainty regarding their capacity for full glycine cleavage. This absence may reflect either genuine metabolic limitation or incomplete genome recovery, as short-read assemblies may miss genes despite high estimated completeness. However, the consistent presence of *glyA* and lactate dehydrogenase genes across Saccharimonadales MAGs supports the potential for glycine-to-serine conversion and subsequent fermentative metabolism to lactate.

Given the high relative abundance of Saccharimonadales in the reactor, this partial pathway suggests that they likely contributed substantially to carbon flux under glycine-fed conditions. Lactate production would enable regeneration of NAD^+ and support redox balance during fermentative metabolism. Although direct lactate measurements were not performed, the genomic potential and dominance of this group are consistent with a fermentative role in the reactor community. In addition, several Saccharimonadales MAGs encoded a lactate permease (*lctP*), which is commonly associated with lactate transport across the membrane. The presence of both lactate dehydrogenase and a lactate transporter supports the potential for lactate production and release, which could make this intermediate available to other community members. In addition to fermentative metabolism, Saccharimonadales MAGs encoded genes associated with glycogen synthesis and degradation (*pgm, glgA, glgC, glgB, glgP*, and *amyA*), indicating the capacity for transient intracellular carbon storage (Wilson et al., 2010).

On the other hand, Saccharimonadales MAGs lacked genes associated with canonical polyhydroxyalkanoate (PHA) biosynthesis (*phaA, phaB*, and *phaC*, among others) and polylactide synthesis (*pct*). Genetic indicators of polyphosphate accumulation, such as the low-affinity inorganic phosphate transporter pit, the high-affinity transporters *pstABCS*, and the polyphosphate kinases (*ppk1* and *ppk2*), were also missing.

Four MAGs affiliated with *Ca.* Phosphoribacter (formerly *Tetrasphaera*) were recovered (Singleton et al., 2022). In contrast to Saccharimonadales, these MAGs encoded a complete glycine cleavage system (*gcvP* (P protein), GCSH (H protein), *gcvT* (T protein), and *lpd* (dihydrolipoyl dehydrogenase), as well as glycine hydroxymethyl transferase (*glyA*) and serine deaminase (*sdaA*), supporting potential direct glycine metabolism (Fig. 3). These genes link glycine transformation to central carbon metabolism through conversion to serine and subsequently to pyruvate.

Although the gene *pct*, associated with polylactide (PLA) synthesis, was not detected, the presence of the *lldEFG* gene cluster (encoding the lactate dehydrogenase complex) indicates the potential for lactate uptake and oxidation in *Ca.* Phosphoribacter. This complex converts lactate to pyruvate while contributing to energy conservation through proton motive force generation (Pinchuk et al., 2009). The coexistence of glycine cleavage and lactate oxidation pathways suggests that *Ca.* Phosphoribacter may utilize glycine directly while also being able to consume fermentation intermediates produced by other members of the community.

Additionally, *Ca.* Phosphoribacter MAGs encoded a comprehensive phosphate transport and accumulation repertoire. They encoded phosphate transport system permease proteins (*pstA, pstC*), phosphate

MAG id	Taxonomic classification	Glycine Cleavage System (GCS)				Serine synthesis			Lactate related genes							Glycogen synthesis and degradation							
		gcvP	*gcvT*	*GCSH*	*lpd*	*glyA*	*serB*	*serC*	*ldh*	*pct*	lldP	*dld*	*lldE*	lldF	*lldG*	*glgC*	*glgA*	*glgB*	*glgM*	*glgE*	*glgP*	*amyA*	*galU*
bin.1	*Ca.* Phosphoribacter sp016710645	1	1	1	1	1	0	0	1	0	0	0	1	1	1	1	0	1	1	1	1	1	0
bin.55	*Ca.* Phosphoribacter sp016715285	1	1	1	1	0	1	1	0	0	0	0	1	1	1	1	0	1	1	1	1	1	1
bin.27	*Saccharimonas*	0	0	0	0	1	0	0	0	0	0	0	0	0	0	0	0	1	0	0	0	1	0
bin.84	Saccharimonadales UBA5946	0	0	0	1	1	0	0	0	0	0	0	0	0	0	0	0	1	0	0	0	1	1
bin.58	Saccharimonadales UBA4665	0	0	0	0	1	0	0	0	0	0	0	0	0	0	0	0	1	0	0	0	1	1
bin.76	Saccharimonadales UBA5946	0	0	0	1	1	0	0	1	0	0	0	0	0	0	0	0	1	0	0	0	1	0
bin.75	Saccharimonadales *GCA-016699895*	0	0	0	0	1	0	0	1	0	0	0	0	0	0	0	0	1	0	0	1	0	0
bin.37	*Ca.* Propionivibrio	1	1	1	1	1	0	1	0	0	0	0	0	0	0	1	1	1	0	0	0	0	0

Genes

MAG id	Taxonomic classification	PolyP metabolism											PHA accumulation					Fermentation						
		pit	*pstA*	*pstB*	*pstC*	pstS	*ppk1*	*ppk2*	*ppx*	*ppgk*	*pap*	*adk*	*phaA*	*phaB*	*phaC*	*phaZ*	*phaJ*	*AckA*	*acs*	*porA*	*porB*	*ald*	*cydA*	*cydB*
bin.1	*Ca.* Phosphoribacter sp016710645	1	1	1	1	1	1	0	1	1	1	1	1	0	1	0	0	0	1	1	1	1	0	0
bin.55	*Ca.* Phosphoribacter sp016715285	1	1	1	1	1	1	0	1	1	1	1	1	0	1	0	0	0	1	1	0	1	1	1
bin.27	*Saccharimonas*	0	0	0	0	0	0	0	0	0	0	0	0	0	0	0	0	1	0	0	0	0	0	0
bin.84	Saccharimonadales UBA5946	0	0	0	0	0	0	0	0	0	0	0	0	0	0	0	0	0	0	0	0	0	0	0
bin.58	Saccharimonadales UBA4665	0	0	0	0	0	0	0	0	0	0	0	0	0	0	0	0	1	0	0	0	0	0	0
bin.76	Saccharimonadales UBA5946	0	0	0	0	0	0	0	0	0	0	0	0	0	0	0	0	0	0	0	0	0	0	0
bin.75	Saccharimonadales *GCA-016699895*	0	0	0	0	0	0	0	0	0	0	0	0	0	0	0	0	0	0	0	0	0	0	0
bin.37	*Ca.* Propionivibrio	1	1	1	1	1	1	0	1	0	1	1	0	0	0	0	0	0	0	0	0	1	1	0

Fig. 3. Presence and absence of central metabolic genes across Ca. Phosphoribacter, Saccharimonadales, and Ca. Propionivibrio MAGs. The top section displays genes involved in the glycine cleavage system (GCS), serine synthesis, lactate-related pathways, and glycogen synthesis and degradation. The bottom section shows genes associated with PolyP metabolism, PHA accumulation, and fermentation. Each row corresponds to a specific MAG, identified by bin number and taxonomic classification. The presence (1) and absence (0) of genes are indicated within the table cells.

transport system ATP-binding protein (*pstB*), phosphate transport system substrate-binding protein (*pstS*), and pit. Other genes involved in the synthesis and hydrolysis, such as exopolyphosphatase (*ppx*), ATP-polyphosphate phosphotransferase (*ppk1*), polyP-AMP phosphotransferase (*pap*), and adenylate kinase (*adk*), were also present. This genetic evidence supports the classification of *Ca*. Phosphoribacter as polyphosphate-accumulating organism (PAO), capable of phosphate metabolism and accumulation.

While the genes encoding acetyl-CoA acetyltransferase (*phaA*) and polyhydroxyalkanoate synthase (*phaC*), both central components of polyhydroxyalkanoate (PHA) biosynthesis, were detected in most *Ca*. Phosphoribacter MAGs, acetoacetyl-CoA reductase (*phaB*) was not identified in any of these genomes. This enzyme catalyzes the reduction step required for canonical PHA production from acetyl-CoA (He and McMahon, 2011). The absence of *phaB* may indicate either incomplete genome recovery or variation from the conventional *phaABC* pathway described in well-characterized PAOs. Similar deviations have been reported in related taxa, suggesting that alternative enzymatic configurations or substrate channeling mechanisms may support PHA formation in *Ca*. Phosphoribacter (Ruiz-Haddad et al., 2024). However, confirmation would require transcriptomic or biochemical validation.

Similarly, analysis of glycogen metabolism genes revealed the presence of glucose-1-phosphate adenylyltransferase (*glgC*) and 1,4-alpha-glucan branching enzyme (*glgB*), but not ADP-glucose glucosyltransferase (*glgA*). Notably, *Ca.* Phosphoribacter MAGs encoded *glgM* and *glgE* genes, which are associated with the alternative glgCME pathway for glycogen synthesis (Elbein et al., 2010). This genomic configuration supports the potential for glycogen biosynthesis through a non-canonical route, consistent with previous reports of metabolic diversity among fermentative PAOs.

The annotated *Ca.* Propionivibrio MAG was also an important member of the community. Although its completeness was lower than that of *Ca.* Phosphoribacter MAGs, it encoded a complete glycine cleavage system (*gcvP*, GCSH, *gcvT*, and *lpd*), together with genes for conversion of glycine to serine and serine to pyruvate. This indicates the capacity for direct glycine metabolism.

In addition, the *Ca.* Propionivibrio MAG encoded genes involved in phosphate transport and polyphosphate metabolism (*pstA, pstC, pstB, pstS, pit, ppx, ppk,* and *adk*), suggesting the potential for phosphorus accumulation. While canonical PHA biosynthesis genes were not detected, glycogen synthesis genes (*glgC, glgA*, and *glgB*) were present. Together, these features indicate that *Ca*. Propionivibrio may function as a PAO-like organism under glycine-fed conditions. However, experimental validation would be required to confirm this activity.

To complement gene presence or absence, we quantified normalized gene abundance (RPKM) by mapping metagenomic reads to the reconstructed MAGs (Table S6). This analysis supported functional partitioning across dominant taxa. Glycine cleavage markers were concentrated in PAO-like MAGs, for example, gcvP (K00281) was detected in *Ca*. Phosphoribacter MAGs (up to 3.94 total RPKM across the two metagenomes) and was not detected in Saccharimonadales MAGs. In contrast, glyA (K00600) showed higher normalized abundance in Saccharimonadales MAGs (up to 65.96 total RPKM) compared with *Ca.* Phosphoribacter MAGs (up to 3.38 total RPKM). Consistent with the gene-content analysis, phosphate transport and polyphosphate metabolism genes were concentrated in *Ca.* Phosphoribacter and *Ca.* Propionivibrio MAGs and were not detected in Saccharimonadales MAGs.

Consistent with the low relative abundance of *Ca*. Accumulibacter observed in the amplicon sequencing and conservative FISH analyses, no *Ca*. Accumulibacter-related MAGs were recovered from the metagenomic dataset.

3.4. Proteomic analysis: expression of glycine and phosphorus metabolism

We used proteomic profiling of pseudo steady-state biomass to evaluate the expression of proteins associated with glycine transformation, phosphorus metabolism, and energy conservation, using the summed area of detected peptides as a proxy for relative protein abundance. We detected proteins mapping to the glycine cleavage system (GCS), and glycine-serine interconversion leading to pyruvate and acetyl CoA (Fig. 4, Kanehisa et al., 2016). Identified KEGG orthologs include glycine dehydrogenase (K00281- K00283, EC 1.4.4.2), amino methyltransferase (K00605, EC 2.1.2.10), glycine cleavage system H protein (K02437), glycine hydroxymethyltransferase (K00600, EC 2.1.2.1), L-serine dehydratase (K01752, EC 4.3.1.17), glycine reductase (K21577), and dihydrolipoamide dehydrogenase (K00382). When we summed the area values for these entries, glycine-related proteins accounted for 7% of the total measured protein area, consistent with measurable expression of glycine-related functions in the reactor community.

Taxonomic assignment of these glycine-related proteins reflected multiple genera in the NCBI-based proteomic framework. Because this taxonomy does not directly correspond to the genome-resolved classifications used elsewhere in this study, we interpret glycine-pathway expression at the community level rather than attributing it to specific MAG-defined taxa (Kleikamp et al., 2023).

Proteins affiliated with *Ca.* Phosphoribacter and *Ca.* Propionivibrio were predominantly associated with glycolysis, dehydrogenase activity, ATP synthesis, and acetyl-CoA metabolism. Together, these assignments suggest that PAO-like taxa were metabolically active and expressed enzymes supporting carbon processing and energy generation under EBPR conditions.

Across the dataset, we detected abundant proteins involved in energy generation, including multiple glycolytic enzymes and ATPase-related proteins. ATPase-related entries accounted for ~ 0.5% of total protein area, consistent with active energy conservation during EBPR operation. While metagenomic reconstruction indicated the presence of phosphate transport and polyphosphate metabolism in PAO-like taxa, polyphosphate kinase and related proteins were not among the most abundant in the proteome dataset, and we therefore interpret proteomic support for polyphosphate cycling primarily through the EBPR genome-resolved potential rather than high protein abundance signals alone.

We detected fewer confidently assigned proteins affiliated with Saccharimonadales, consistent with their reduced genome size and limited reference representation in current protein databases (Albertsen et al., 2013; Peñalver et al., 2024). Overcoming these obstacles may require optimized sample preparation methods (Carbonara et al., 2021).

4. Discussion

4.1. The impact of glycine on EBPR systems and its use by the PAO community

Previous studies investigating glycine in EBPR systems have reported variable outcomes. Nguyen et al. (2015) demonstrated that glycine can induce anaerobic phosphorus release followed by aerobic uptake in *Tetrasphaera*-dominated systems, suggesting intracellular storage and subsequent oxidation. This release was particularly notable, as glycine exhibited one of the highest phosphorus release rates, second only to acetate. Similar results were reported by Liu et al. (2022), who observed high levels of anaerobic glycine storage and aerobic metabolization in *Tetrasphaera*-dominated communities during phosphorus removal.

However, other studies have shown that although glycine can be metabolized, certain PAO systems do not utilize it efficiently (Qiu et al., 2020; Tian et al., 2022). For example, Qiu et al. (2020) reported that glycine-induced phosphorus release was poorly coupled with carbon uptake in *Ca.* Accumulibacter. In that study, glycine exhibited a lower anaerobic phosphorus release rate (5.9 mg P g^{-1} MLSS h^{-1}) than acetate and other amino acids, such as aspartate and glutamate, highlighting its distinct kinetics and lower substrate preference. The carbon uptake rate was also low (1.56 mg C g^{-1} MLSS h^{-1}), even though the metatranscriptomic analysis of one of their enriched cultures showed the

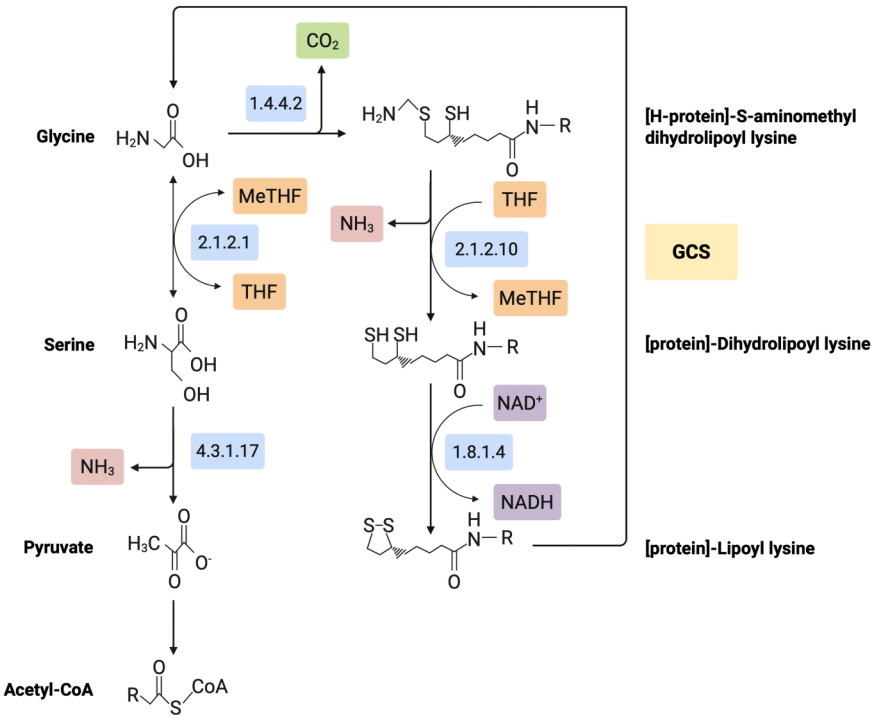

Fig. 4. Glycine transformation route supported by proteomic evidence in pseudo steady-state reactor biomass. The pathway schematic summarizes the glycine cleavage system (GCS) and the conversion of glycine to serine and subsequently to acetyl-CoA. Enzyme EC numbers and key cofactors (methylene-THF/THF and NAD+/NADH) are shown. Functional annotation and KEGG orthology assignment were performed using BlastKOALA (Kanehisa et al., 2016). Proteins annotated to glycine transformation steps accounted for 7% of the total measured protein area.

expression of glycine cleavage operons. Tian et al. (2022) also reported glycine-induced phosphorus release under anaerobic conditions. Nonetheless, the enriched microbiome did not take up phosphorus in the subsequent oxic stage, and the meta-transcriptomic analysis indicated potential barriers to glycine metabolism. Given its substantial P/C release ratio of 4.67 mol P mol^{-1} C, the authors propose glycine as a viable means for recovering phosphorus from P-enriched waste sludge. Hence, both studies align in underscoring that, despite glycine's apparent limited efficiency in enhanced biological phosphorus removal, its role demands further scrutiny for potential contributions to selective taxonomic enrichment, emphasizing its relevance in the research of wastewater treatment processes.

In the present study, glycine supported EBPR activity, as evidenced by complete anaerobic DOC consumption, a strong negative association between DOC depletion and phosphorus release, and subsequent aerobic phosphorus uptake. However, the kinetics differed from those typically reported for acetate-fed systems. The anaerobic phosphate release rate (3.7 mg PO_4-P g^{-1} VSS h^{-1}) and aerobic uptake rate (3.6 mg PO_4-P g^{-1} VSS h^{-1}) were lower than rates commonly observed in acetate-enriched EBPR reactors, where release rates commonly exceed 10 mg PO_4-P g^{-1} VSS h^{-1} (Smolders et al., 1994; Ziliani et al., 2023). These differences indicate that although glycine can support polyphosphate cycling, the metabolic turnover proceeds with slower kinetics compared to readily fermentable volatile fatty acids.

Despite slower kinetics, the overall stoichiometry was consistent with EBPR behavior typically attributed to PAO activity. The DOC:P removal ratio (100:9.9) was close to the classical value reported for EBPR systems (100:8) (Smolders et al., 1994). The net P removal per cycle (20 mg PO_4-P L^{-1}) is comparable to laboratory-scale EBPR systems fed with mixed carbon sources (Crnek et al., 2024; Yang et al., 2018; Ziliani et al., 2023). These findings suggest that glycine can sustain functional EBPR, although performance fluctuated during operation and remained kinetically distinct from VFA-fed systems.

The observed differences may be related to substrate-specific metabolic capacities. In acetate-fed systems, VFAs are directly taken up and stored by conventional PAOs, enabling rapid anaerobic carbon assimilation and phosphate release. In contrast, glycine requires intracellular conversion to central metabolites and, depending on the community structure, may involve fermentative intermediates before assimilation. Such additional steps could be contributing to the different release-uptake morphology and slower apparent kinetics observed here.

In addition to serving as a carbon source, glycine also provides nitrogen, and its degradation releases ammonium. In our system, nitrification was inhibited by allylthiourea (ATU), and nitrate was not detected during operation, indicating negligible nitrification activity. Under the controlled pH and temperature conditions applied, ammonium is expected to remain predominantly in the NH_4^+ form, and nitrogen transformations are unlikely to have been a major driver of the observed community shifts.

4.2. *Community composition under glycine-fed conditions*

Our 16S rRNA gene amplicon sequencing analysis showed a community restructuring during reactor operation, as expected for enrichment under selective SBR conditions. Saccharimonadales became the dominant order (~ 50% relative abundance), while *Ca.* Phosphoribacter and *Ca.* Propionivibrio were also enriched. In contrast, *Ca.* Accumulibacter remained at low abundance based on both 16S rRNA gene amplicon sequencing and conservative FISH quantification using probe PAO 651 (Albertsen et al., 2016). This is consistent with previous studies indicating that *Ca.* Accumulibacter does not efficiently compete for amino acids under certain conditions (Marques et al., 2017; Qiu et al., 2020).

Marques et al. (2017) reported that in a mixed PAO community composed mainly of *Tetrasphaera* and *Ca.* Accumulibacter, the latter prospered on the fermentation products generated by *Tetrasphaera.* In our study, the genomic potential reconstructed from MAGs suggests a similar ecological partition may have occurred, although involving

different taxa. Saccharimonadales dominated the community and, based on MAG reconstruction, encoded *glyA* and lactate dehydrogenase genes, supporting potential conversion of glycine to serine and subsequently to lactate (Fig. 5). Several Saccharimonadales MAGs also encoded a lactate permease (*lctP*), indicating the genetic capacity for lactate transport across the membrane. Together, these features align with fermentative carbon processing during the anaerobic phase of reactor operation. Previous studies have reported lactate formation from amino acid metabolism under similar conditions (Qiu et al., 2020; Tian et al., 2022). However, canonical glycine cleavage system genes were not detected in these MAGs, introducing uncertainty regarding the extent and mechanism of glycine transformation by this group.

In contrast, *Ca.* Phosphoribacter and *Ca.* Propionivibrio MAGs encoded complete glycine cleavage systems and genes linking glycine metabolism to central carbon pathways. *Ca.* Phosphoribacter has previously been reported as a fermentative PAO capable of utilizing amino acids and sugars, and our MAGs confirm the presence of both glycine metabolism genes and polyphosphate-accumulating pathways (Fig. 5) (Ruiz-Haddad et al., 2024; Singleton et al., 2022). The presence of lactate dehydrogenase complex genes (lldEFG) further supports the potential for lactate oxidation, suggesting metabolic flexibility.

Taken together, these findings indicate that glycine metabolism potential was distributed across multiple enriched populations, and that phosphorus removal was likely supported by both direct glycine metabolism by PAO-like organisms and transformation products generated by other community members. One possible scenario is that Saccharimonadales contributed to partial glycine fermentation, generating intermediates such as lactate, while PAO-like organisms directly metabolized glycine and consumed fermentation products. However, because glycine and lactate were not directly quantified during the cycle studies, and MAG-based inference does not resolve metabolic flux, the relative contribution of each group to glycine turnover cannot be definitively determined. The RPKM-based gene abundance analysis was consistent with this partitioning, with glycine cleavage and polyphosphate metabolism genes concentrated in PAO-like MAGs (*Ca.* Phosphoribacter and *Ca.* Propionivibrio) and fermentative glycine-related genes more prominent in Saccharimonadales.

The absence of a distinct DOC peak attributable to lactate accumulation during the cycle studies may reflect rapid turnover, as reported for fermentative intermediates in mixed microbial systems (Finke et al., 2007; Pinchuk et al., 2009). Nevertheless, without targeted lactate measurements, this interpretation remains tentative.

Importantly, phosphorus removal was achieved despite the low abundance of *Ca.* Accumulibacter, indicating that PAO-like taxa

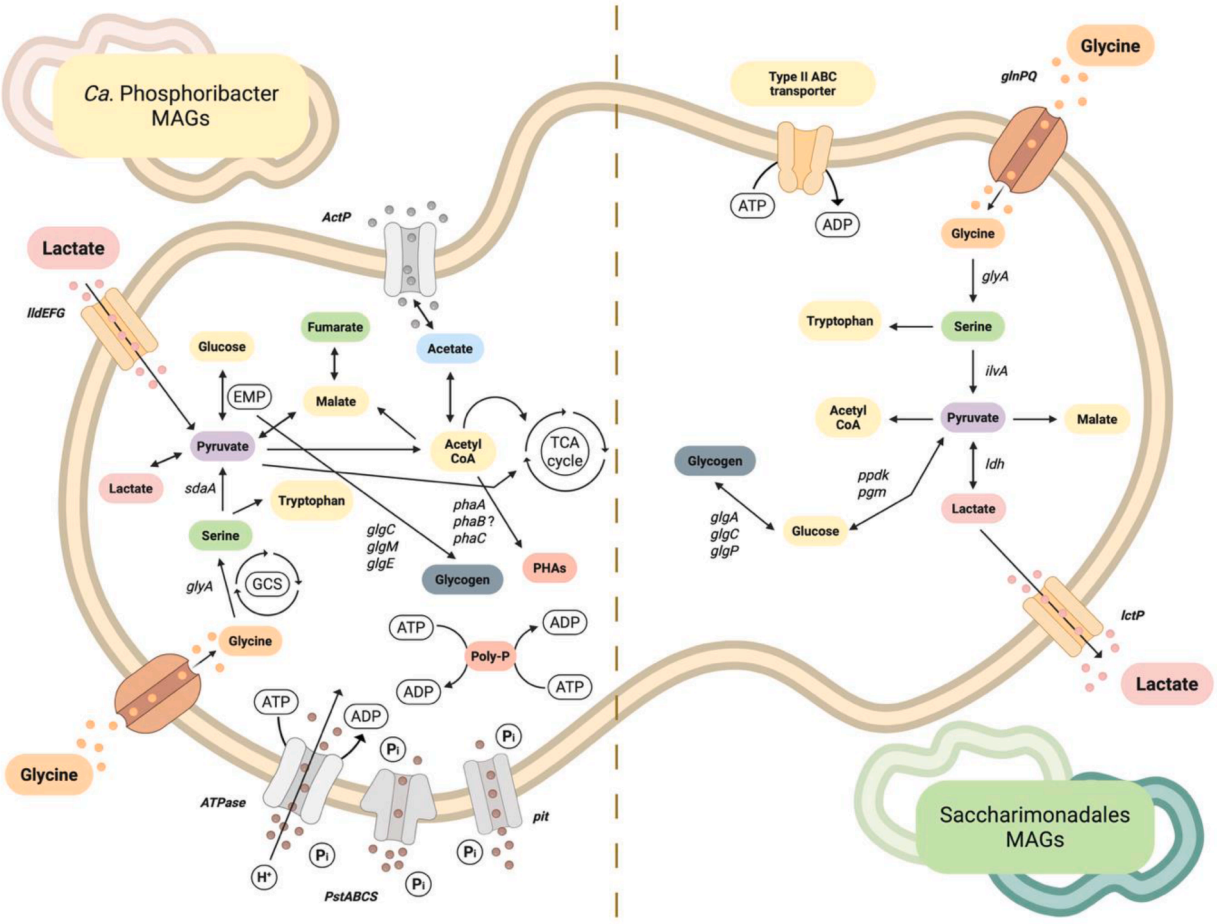

Fig. 5. Proposed metabolic pathways reconstructed from Saccharimonadales and *Ca.* Phosphoribacter MAGs. The schematic summarizes genomic potential related to glycine uptake and transformation, central carbon metabolism, lactate production and consumption, glycogen metabolism, and polyphosphate accumulation. Pathways shown reflect annotated gene presence and represent potential metabolic capabilities only. Quantitative fluxes or expression levels are not implied. Genes marked with a question mark (?) were not detected in the corresponding MAG. Saccharimonadales MAGs encoded glycine ABC transporters (*glnPQ*), glycine hydroxymethyltransferase (*glyA*), serine deaminase (*sdaA*), L-serine/L-threonine dehydratase (*ilvA*), lactate dehydrogenase (*ldh*), lactate permease (*lctP*), pyruvate phosphate dikinase (*ppdk*), and glycogen metabolism genes (*glgA, glgP*). Canonical glycine cleavage system genes were not detected. *Ca.* Phosphoribacter MAGs encoded a complete glycine cleavage system (GCS) (*gcvP, gcvT, GCSH, lpd*), the lactate oxidation complex (lldEFG), genes associated with phosphate transport and polyphosphate metabolism (*pit, pstABCS, ppk, ppx*), and genes involved in polyhydroxyalkanoate and glycogen biosynthesis pathways (*phaA, phaC, glgC, glgB, glgM, glgE*), while *phaB* and *glgA* were not detected.

supported EBPR activity under glycine-fed conditions. The enrichment of *Ca.* Phosphoribacter and *Ca.* Propionivibrio, together with their encoded polyphosphate accumulation pathway genes, supports their functional relevance in the system. Proteomic profiling further supported community-level expression of glycine transformation proteins and broad expression of energy metabolism proteins across different taxa.

4.3. Analysis of Saccharimonadales and Ca. Phosphoribacter genomes reveals previously undescribed Saccharimonadales lineages

Our study annotated four MAGs from the order Saccharimonadales, each with a completeness level exceeding 97%. We performed an average nucleotide identity (ANI) test to contextualize our findings, comparing our MAGs to other publicly available Saccharimonadales genomes (Fig. 6A). Analyzing the results, it became clear that only bin.75 Saccharimonadales GCA-016699895 shows distant similarity to an existing genome (GCA_032229385.1) with an ANI of 83%. These values fall below the commonly accepted species threshold, indicating that these MAGs likely represent previously undescribed Saccharimonadales lineages.

The recovery of high-quality Saccharimonadales genomes, coupled with their dominance in the community, expands current genomic knowledge of this order in engineered systems and highlights their potential ecological relevance under amino acid-fed conditions.

The results for the two *Ca.* Phosphoribacter MAGs, on the other hand, showed that bin.1 *Ca.* Phosphoribacter sp016710645 likely represents the same species as Pbr5_Hjor_b81 -Phosphoribacter sp016710645 (ANI of 99.37%) and bin.55 *Ca.* Phosphoribacter sp016715285 showed the highest ANI value of 99.32% with Pbr6_Mari_b41 -Phosphoribacter sp016715285, also suggesting species-level similarity (Fig. 6B). Both of these MAGs were reported in the research by Singleton et al. (2022), and strengthen the interpretation that *Ca.* Phosphoribacter populations enriched in our reactor correspond to known fermentative PAO-like taxa.

To provide a broader phylogenetic context, representative canonical PAO genomes were included in the reconstruction. The *Ca.* Phosphoribacter MAGs clustered distinctly from *Ca.* Accumulibacter lineages, reinforcing that the PAO-like populations enriched in this reactor differ phylogenetically from classical *Ca.* Accumulibacter-dominated EBPR systems. This supports the interpretation that glycine-driven phosphorus removal in our system was associated primarily with fermentative PAO-related taxa rather than conventional PAO populations.

5. Conclusions

Glycine supported anaerobic phosphorus release and subsequent aerobic uptake in a sequencing batch reactor operated for over 90 days, although removal performance fluctuated during operation, and release-uptake kinetics were slower than those typically reported for VFA-fed systems. The microbial community that developed under glycine-fed conditions differed from classical acetate-driven EBPR enrichments, with Saccharimonadales dominating and *Ca.* Accumulibacter remaining at low abundance.

Genome-resolved analyses showed that glycine metabolism potential was distributed across fermentative and PAO-like taxa. *Ca.* Phosphoribacter and *Ca.* Propionivibrio encoded complete glycine cleavage systems and polyphosphate metabolism genes, supporting their role in phosphorus accumulation. In contrast, Saccharimonadales encoded genes consistent with partial glycine transformation and fermentative metabolism but lacked canonical polyphosphate pathways.

Together, these results suggest that glycine-driven EBPR can be

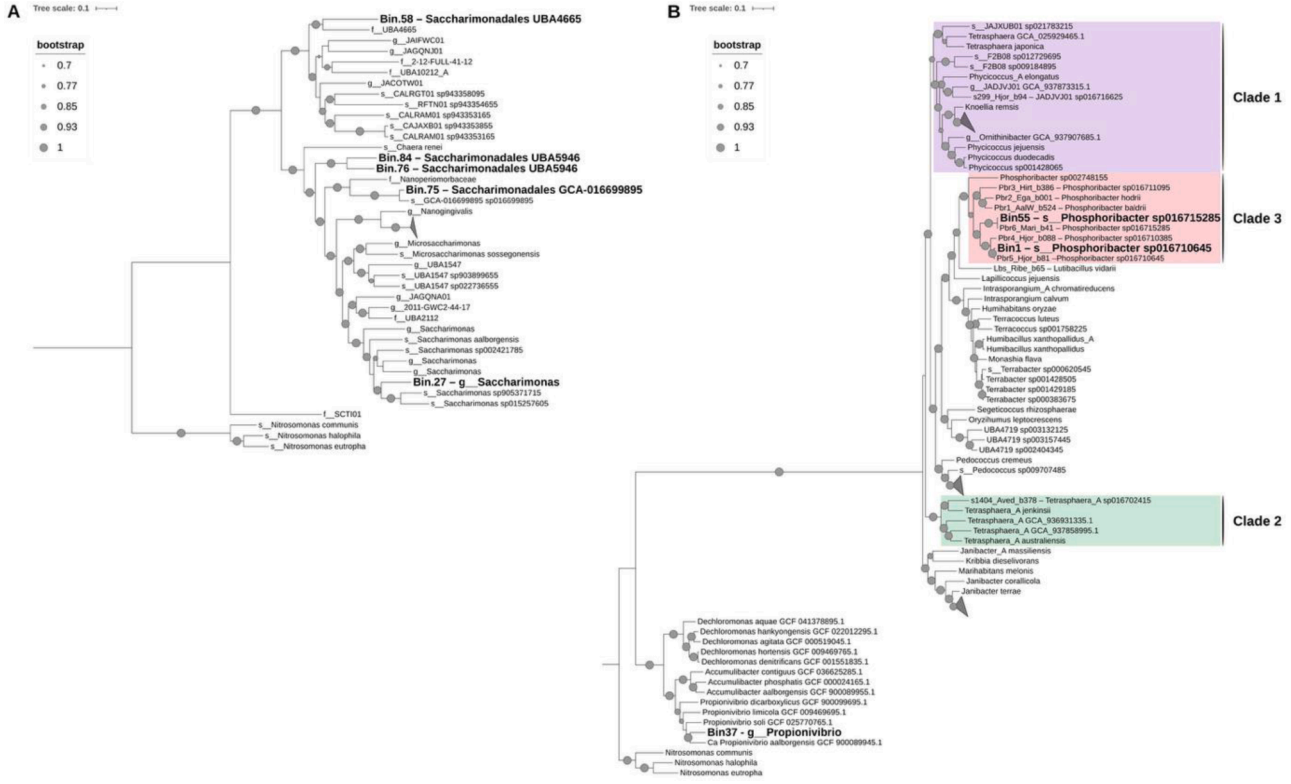

Fig. 6. A. Phylogenetic tree showing the position of metagenome-assembled genomes (MAGs) affiliated with the Saccharimonadales order (*i.e.*, bin_58, bin_84, bin_76, bin_75, and bin_27). B. Phylogenetic placement of Ca. Phosphoribacter MAGs (bin_1 and bin_55) relative to representatives of the historical Tetrasphaera clades, shown alongside canonical PAO lineages for phylogenetic context. The Ca. Propionivibrio (bin_37) MAG is included as a PAO-related reference but does not belong to the Tetrasphaera clade framework. Genomes with $\geq$ 50% completeness were included in the reconstruction; the Ca. Propionivibrio MAG (completeness $<$ 50%) is shown for contextual comparison and its phylogenetic placement should therefore be interpreted cautiously.

sustained under the conditions tested by a community in which carbon transformation and phosphorus accumulation functions are partitioned across multiple taxa. However, the precise metabolic routes and metabolite exchange dynamics remain to be resolved through targeted metabolite and activity-based measurements.

Data availability

Supporting data are desposited in the Eawag Research Data Institutional Repository (https://opendata.eawag.ch/).

CRediT authorship contribution statement

Agustina Ziliani: Writing – original draft, Visualization, Methodology, Investigation, Formal analysis. **Patricia Bovio-Winkler:** Writing – review & editing, Visualization, Formal analysis. **Martin Pabst:** Writing – review & editing, Formal analysis. **Angela Cabezas:** Writing – review & editing. **Claudia Etchebehere:** Writing – review & editing. **Hector A. Garcia:** Conceptualization. **Carlos M. López-Vázquez:** Supervision, Conceptualization. **Damir Brdjanovic:** Supervision. **Mark C. M. van Loosdrecht:** Writing – review & editing, Supervision, Conceptualization. **Francisco J. Rubio-Rincón:** Writing – original draft, Supervision, Conceptualization.

Declaration of competing interest

The authors declare that they have no known competing financial interests or personal relationships that could have appeared to influence the work reported in this paper.

Acknowledgments

This work was supported by the National Agency for Research and Innovation (ANII, Uruguay).

Supplementary materials

Supplementary material associated with this article can be found, in the online version, at doi:10.1016/j.watres.2026.126057.

References

Albertsen, M., McIlroy, S.J., Stokholm-Bjerregaard, M., Karst, S.M., Nielsen, P.H., 2016. "*Candidatus Propionivibrio aalborgensis*": a novel glycogen accumulating organism abundant in full-scale enhanced biological phosphorus removal plants. Front. Microbiol. 7. https://doi.org/10.3389/fmicb.2016.01033.

Albertsen, M., Philip, H., Skarshewski, A., Nielsen, K., Tyson, G., Nielsen, P., 2013. Genome sequences of rare, uncultured bacteria obtained by differential coverage binning of multiple metagenomes. Nat. Biotechnol. 31. https://doi.org/10.1038/nbt.2579.

APHA AWWA WEF, 2005. Standard Methods for the Examination of Water and Wastewater. APHA-AWWA-WEF, Washington, D.C.

Barnard, J.L., Dunlap, P., Steichen, M., 2017. Rethinking the mechanisms of biological phosphorus removal. Water Environ. Res. 89, 2043–2054. https://doi.org/10.2175/106143017x15051465919010.

Bowers, R.M., Kyrpides, N.C., Stepanauskas, R., Harmon-Smith, M., Doud, D., Reddy, T. B.K., Schulz, F., Jarett, J., Rivers, A.R., Eloe-Fadrosh, E.A., Tringe, S.G., Ivanova, N. N., Copeland, A., Clum, A., Becraft, E.D., Malmstrom, R.R., Birren, B., Podar, M., Bork, P., Weinstock, G.M., Garrity, G.M., Dodsworth, J.A., Yooseph, S., Sutton, G., Glöckner, F.O., Gilbert, J.A., Nelson, W.C., Hallam, S.J., Jungbluth, S.P., Ettema, T.J. G., Tighe, S., Konstantinidis, K.T., Liu, W.-T., Baker, B.J., Rattei, T., Eisen, J.A., Hedlund, B., McMahon, K.D., Fierer, N., Knight, R., Finn, R., Cochrane, G., Karsch-Mizrachi, I., Tyson, G.W., Rinke, C., Kyrpides, N.C., Schriml, L., Garrity, G.M., Hugenholtz, P., Sutton, G., Yilmaz, P., Meyer, F., Glöckner, F.O., Gilbert, J.A., Knight, R., Finn, R., Cochrane, G., Karsch-Mizrachi, I., Lapidus, A., Meyer, F., Yilmaz, P., Parks, D.H., Murat Eren, A., Schriml, L., Banfield, J.F., Hugenholtz, P., Woyke, T., Consortium, T.G.S., 2017. Minimum information about a single amplified genome (MISAG) and a metagenome-assembled genome (MIMAG) of bacteria and archaea. Nat. Biotechnol. 35, 725–731. https://doi.org/10.1038/nbt.3893.

Bunce, J.T., Ndam, E., Ofiteru, I.D., Moore, A., Graham, D.W., 2018. A review of phosphorus removal technologies and their applicability to small-scale domestic wastewater treatment systems. Front. Environ. Sci. 6. https://doi.org/10.3389/fenvs.2018.00008.

Callahan, B.J., McMurdie, P.J., Rosen, M.J., Han, A.W., Johnson, A.J.A., Holmes, S.P., 2016. DADA2: high-resolution sample inference from Illumina amplicon data. Nat. Methods 13, 581–583. https://doi.org/10.1038/nmeth.3869.

Carbonara, K., Andonovski, M., Coorssen, J.R., 2021. Proteomes are of proteoforms: embracing the complexity. Proteomes 9, 38. https://doi.org/10.3390/proteomes9030038.

Chaumeil, P.-A., Mussig, A.J., Hugenholtz, P., Parks, D.H., 2020. GTDB-Tk: a toolkit to classify genomes with the genome taxonomy database. Bioinformatics 36, 1925–1927. https://doi.org/10.1093/bioinformatics/btz848.

Confer, D., Logan, B., Aiken, B., Kirchman, D., 1995. Measurement of dissolved free and combined amino acids in unconcentrated wastewaters using high performance liquid chromatography. Water Environ. Res. 67, 118–125. https://doi.org/10.2175/106143095X131268.

Crnek, V., Tomić, V.M., Vuković, M., Ćurko, J., Matošić, M., 2024. Influence of high acetate concentrations on enhanced biological phosphorus removal. Int. J. Environ. Sci. Technol. https://doi.org/10.1007/s13762-024-05555-2.

Crocetti, G.R., Banfield, J.F., Keller, J., Bond, P.L., Blackall, L.L., 2002. Glycogen-accumulating organisms in laboratory-scale and full-scale wastewater treatment processes. Microbiology (N. Y). 148, 3353–3364. https://doi.org/10.1099/00221287-148-11-3353.

Crocetti, G.R., Hugenholtz, P., Bond, P.L., Schuler, A., Keller, J., Jenkins, D., Blackall, L. L., 2000. Identification of polyphosphate-accumulating organisms and design of 16S rRNA-directed probes for their detection and quantitation. Appl. Environ. Microbiol. 66, 1175–1182. https://doi.org/10.1128/AEM.66.3.1175-1182.2000.

Dueholm, M.K.D., Nierychlo, M., Andersen, K.S., Rudkjøbing, V., Knutsson, S., Arriaga, S., Bakke, R., Boon, N., Bux, F., Christensson, M., Chua, A.S.M., Curtis, T.P., Cytryn, E., Erijman, L., Etchebehere, C., Fatta-Kassinos, D., Frigon, D., Garcia-Chaves, M.C., Gu, A.Z., Horn, H., Jenkins, D., Kreuzinger, N., Kumari, S., Lanham, A., Law, Y., Leiknes, T.O., Morgenroth, E., Muszyński, A., Petrovski, S., Pijuan, M., Pillai, S.B., Reis, M.A.M., Rong, Q., Rossetti, S., Seviour, R., Tooker, N., Vainio, P., van Loosdrecht, M.C.M., Vikraman, R., Wanner, J., Weissbrodt, D., Wen, X., Zhang, T., Albertsen, M., Nielsen, P.H., 2022. MiDAS 4: a global catalogue of full-length 16S rRNA gene sequences and taxonomy for studies of bacterial communities in wastewater treatment plants. Nat. Commun. 13. https://doi.org/10.1038/s41467-022-29438-7.

Elahinik, A., Haarsma, M., Abbas, B., Pabst, M., Xevgenos, D., van Loosdrecht, M.C.M., Pronk, M., 2022. Glycerol conversion by aerobic granular sludge. Water Res. 227, 119340. https://doi.org/10.1016/j.watres.2022.119340.

Elahinik, A., Li, L., Pabst, M., Abbas, B., Xevgenos, D., van Loosdrecht, M.C.M., Pronk, M., 2023. Aerobic granular sludge phosphate removal using glucose. Water Res. 247, 120776. https://doi.org/10.1016/j.watres.2023.120776.

Elbein, A.D., Pastuszak, I., Tackett, A.J., Wilson, T., Pan, Y.T., 2010. Last step in the conversion of trehalose to glycogen: a mycobacterial enzyme that transfers maltose from maltose 1-phosphate to glycogen. J. Biol. Chem. 285, 9803–9812. https://doi.org/10.1074/jbc.M109.033944.

Finke, N., Vandieken, V., Jørgensen, B.B., 2007. Acetate, lactate, propionate, and isobutyrate as electron donors for iron and sulfate reduction in Arctic marine sediments, Svalbard. FEMS Microbiol. Ecol. 59, 10–22. https://doi.org/10.1111/j.1574-6941.2006.00214.x.

He, S., McMahon, K.D., 2011. Microbiology of '*Candidatus* Accumulibacter' in activated sludge. Microb. Biotechnol. 4, 603–619. https://doi.org/10.1111/j.1751-7915.2011.00248.x.

Herlemann, D.P.R., Labrenz, M., Jürgens, K., Bertilsson, S., Waniek, J.J., Andersson, A.F., 2011. Transitions in bacterial communities along the 2000 km salinity gradient of the Baltic Sea. ISME J. 5, 1571–1579. https://doi.org/10.1038/ismej.2011.41.

Kanehisa, M., Goto, S., 2000. KEGG: kyoto encyclopedia of genes and genomes. Nucleic Acids Res. 28, 27–30. https://doi.org/10.1093/nar/28.1.27.

Kanehisa, M., Sato, Y., Morishima, K., 2016. BlastKOALA and GhostKOALA: KEGG tools for functional characterization of genome and metagenome sequences. J. Mol. Biol. 428, 726–731. https://doi.org/10.1016/j.jmb.2015.11.006.

Kawakoshi, A., Nakazawa, H., Fukada, J., Sasagawa, M., Katano, Y., Nakamura, S., Hosoyama, A., Sasaki, H., Ichikawa, N., Hanada, S., Kamagata, Y., Nakamura, K., Yamazaki, S., Fujita, N., 2012. Deciphering the genome of polyphosphate accumulating Actinobacterium *Microlunatus phosphovorus*. DNA Res. 19, 383–394. https://doi.org/10.1093/dnares/dss020.

Kleikamp, H.B.C., Grouzdev, D., Schaasberg, P., van Valderen, R., van der Zwaan, R., van de Wijgaart, R., Lin, Y., Abbas, B., Pronk, M., van Loosdrecht, M.C.M., Pabst, M., 2023. Metaproteomics, metagenomics and 16S rRNA sequencing provide different perspectives on the aerobic granular sludge microbiome. Water Res. 246, 120700. https://doi.org/10.1016/j.watres.2023.120700.

Liu, H., Zeng, W., Meng, Q., Fan, Z., Peng, Y., 2022. Phosphorus removal performance, intracellular metabolites and clade-level community structure of *Tetrasphaera*-dominated polyphosphate accumulating organisms at different temperatures. Sci. Total Environ. 842, 156913. https://doi.org/10.1016/j.scitotenv.2022.156913.

Marques, R., Santos, J., Nguyen, H., Carvalho, G., Noronha, J.P., Nielsen, P.H., Reis, M.A. M., Oehmen, A., 2017. Metabolism and ecological niche of *Tetrasphaera* and *Ca.* Accumulibacter in enhanced biological phosphorus removal. Water Res. 122, 159–171. https://doi.org/10.1016/j.watres.2017.04.072.

Nguyen, H.T.T., Kristiansen, R., Vestergaard, M., Wimmer, R., Nielsen, P.H., 2015. Intracellular accumulation of glycine in polyphosphate-accumulating organisms in activated sludge, a novel storage mechanism under dynamic anaerobic-aerobic conditions. Appl. Environ. Microbiol. 81, 4809–4818. https://doi.org/10.1128/AEM.01012-15.

Nguyen, H.T.T., Le, V.Q., Hansen, A.A., Nielsen, J.L., Nielsen, P.H., 2011. High diversity and abundance of putative polyphosphate-accumulating *Tetrasphaera*-related

bacteria in activated sludge systems. FEMS Microbiol. Ecol. 76, 256–267. https://doi.org/10.1111/j.1574-6941.2011.01049.x.

Nielsen, P.H., Saunders, A.M., Hansen, A.A., Larsen, P., Nielsen, J.L., 2012. Microbial communities involved in enhanced biological phosphorus removal from wastewater—a model system in environmental biotechnology. Curr. Opin. Biotechnol. 23, 452–459. https://doi.org/10.1016/j.copbio.2011.11.027.

Oyserman, B.O., Noguera, D.R., del Rio, T.G., Tringe, S.G., McMahon, K.D., 2016. Metatranscriptomic insights on gene expression and regulatory controls in *Candidatus Accumulibacter phosphatis*. ISME J. 10, 810–822. https://doi.org/10.1038/ismej.2015.155.

Parks, D.H., Chuvochina, M., Chaumeil, P.-A., Rinke, C., Mussig, A.J., Hugenholtz, P., 2020. A complete domain-to-species taxonomy for bacteria and archaea. Nat. Biotechnol. 38, 1079–1086. https://doi.org/10.1038/s41587-020-0501-8.

Parks, D.H., Imelfort, M., Skennerton, C.T., Hugenholtz, P., Tyson, G.W., 2015. CheckM: assessing the quality of microbial genomes recovered from isolates, single cells, and metagenomes. Genome Res. 25, 1043–1055. https://doi.org/10.1101/gr.186072.114.

Peñalver, M., Paradela, A., Palacios-Cuéllar, C., Pucciarelli, M.G., García-del Portillo, F., 2024. Experimental evidence of d-glutamate racemase activity in the uncultivated bacterium Candidatus *Saccharimonas aalborgensis*. Environ. Microbiol. 26, e16621. https://doi.org/10.1111/1462-2920.16621.

Pinchuk, G.E., Rodionov, D.A., Yang, C., Li, X., Osterman, A.L., Dervyn, E., Geydebrekht, O.V., Reed, S.B., Romine, M.F., Collart, F.R., Scott, J.H., Fredrickson, J.K., Beliaev, A.S., 2009. Genomic reconstruction of *Shewanella oneidensis* MR-1 metabolism reveals a previously uncharacterized machinery for lactate utilization. Proc. Natl. Acad. Sci. U.S.A. 106, 2874–2879. https://doi.org/10.1073/pnas.0806798106.

Qiu, G., Liu, X., Saw, N.M.M.T., Law, Y., Zuniga-Montanez, R., Thi, S.S., Ngoc Nguyen, T. Q., Nielsen, P.H., Williams, R.B.H., Wuertz, S., 2020. Metabolic traits of *Candidatus Accumulibacter clade* IIF strain SCELSE-1 using amino acids as carbon sources for enhanced biological phosphorus removal. Environ. Sci. Technol. 54, 2448–2458. https://doi.org/10.1021/acs.est.9b02901.

Rubio-Rincón, F.J., Welles, L., Lopez-Vazquez, C.M., Abbas, B., van Loosdrecht, M.C.M., Brdjanovic, D., 2019. Effect of lactate on the microbial community and process performance of an EBPR system. Front. Microbiol. 10, 1–11. https://doi.org/10.3389/fmicb.2019.00125.

Rubio-Rincón, F.J., Welles, L., Lopez-Vazquez, C.M., Nierychlo, M., Abbas, B., Geleijnse, M., Nielsen, P.H., van Loosdrecht, M.C.M., Brdjanovic, D., 2017. Long-term effects of sulphide on the enhanced biological removal of phosphorus: the symbiotic role of *Thiothrix caldifontis*. Water Res. 116, 53–64. https://doi.org/10.1016/J.WATRES.2017.03.017.

Ruiz-Haddad, L., Ali, M., Pronk, M., van Loosdrecht, M.C.M., Saikaly, P.E., 2024. Demystifying polyphosphate-accumulating organisms relevant to wastewater treatment: a review of their phylogeny, metabolism, and detection. Environ. Sci. Ecotechnol. 21, 100387. https://doi.org/10.1016/j.ese.2024.100387.

Singleton, C.M., Petriglieri, F., Wasmund, K., Nierychlo, M., Kondrotaite, Z., Petersen, J. F., Peces, M., Dueholm, M.S., Wagner, M., Nielsen, P.H., 2022. The novel genus, '*Candidatus* Phosphoribacter', previously identified as *Tetrasphaera*, is the dominant polyphosphate accumulating lineage in EBPR wastewater treatment plants worldwide. ISME J. 16, 1605–1616. https://doi.org/10.1038/s41396-022-01212-z.

Smolders, G.J.F., van der Meij, J., van Loosdrecht, M.C.M., Heijnen, J.J., 1994. Model of the anaerobic metabolism of the biological phosphorus removal process: stoichiometry and pH influence. Biotechnol. Bioeng. 43, 461–470. https://doi.org/10.1002/bit.260430605.

Smolders, G.J.F., van Loosdrecht, M.C.M., Heijnen, J.J., 1995. A metabolic model for the biological phosphorus removal process. Water Sci. Technol. 31, 79–93. https://doi.org/10.1016/0273-1223(95)00182-M.

Thomson, R., Close, K., Riley, A., Batstone, D.J., Oehmen, A., 2025. Metabolic modelling of anaerobic amino acid uptake and storage by fermentative polyphosphate accumulating organisms. Water Res. 280. https://doi.org/10.1016/j.watres.2025.123512.

Tian, Y., Chen, H., Chen, L., Deng, X., Hu, Z., Wang, C., Wei, C., Qiu, G., Wuertz, S., 2022. Glycine adversely affects enhanced biological phosphorus removal. Water Res. 209, 117894. https://doi.org/10.1016/j.watres.2021.117894.

Wilson, W.A., Roach, P.J., Montero, M., Baroja-Fernández, E., Muñoz, F.J., Eydallin, G., Viale, A.M., Pozueta-Romero, J., 2010. Regulation of glycogen metabolism in yeast and bacteria. FEMS Microbiol. Rev. 34, 952–985. https://doi.org/10.1111/j.1574-6976.2010.00220.x.

Yang, G., Wang, D., Yang, Q., Zhao, J., Liu, Y., Wang, Q., Zeng, G., Li, X., Li, H., 2018. Effect of acetate to glycerol ratio on enhanced biological phosphorus removal. Chemosphere 196, 78–86. https://doi.org/10.1016/j.chemosphere.2017.12.167.

Ziliani, A., Bovio-Winkler, P., Cabezas, A., Etchebehere, C., Garcia, H.A., López-Vázquez, C.M., Brdjanovic, D., van Loosdrecht, M.C.M., Rubio-Rincón, F.J., 2023. Putative metabolism of *Ca.* Accumulibacter via the utilization of glucose. Water Res. 229, 119446. https://doi.org/10.1016/j.watres.2022.119446.